Chapter 12
Mapping Marine Macrophytes along the Atlantic Coast of Tierra Del Fuego (Argentina) by Remote Sensing

Sandra E. Torrusio

A discontinuous series of rocky formations with variable dimensions exist along the intertidal zones in the eastern coast of Tierra del Fuego, Argentina, where an abundance of marine macrophytes grow, such as *Macrocystis pyrifera* forming subaquatic “forests”. This large amount of algae forms true fauna reservoirs and provide potential stocks for deriving industrial algae products. The purpose of this study is to map the undersea fauna resources by remote sensing and to evaluate the utilities of different remote sensors given the frequent cloud cover and the winter days with low sunlight. The data used include satellite imagery from Landsat, SAC-C, Aster, Radarsat and QuickBird, as well as aerial photographs and maps. We co-register them before actual mapping the algae distribution using different methods. The final maps illustrate the algae distribution and temporal change, which can be useful for managing the coastal environment and resources.

12.1 Introduction

The intertidal and subtidal environments with rocky bottom in template and subpolar seas are dominated by brown algae associations (Dayton 1985). These marine macrophyte communities are constantly exposed to tidal changes. The algae communities are economically important due to its alginate contents; the phycocolloids found in algae are useful to different industries, such as textile, food, paper, dental and pharmaceutical, soldering, among others (Rees 1986). The fucales, laminariales and durvilleales are used to extract alginates all over the world. In South America the main exploited genus are *Lessonia spp* and *Macrocystis spp*, and both constitute the most extensive high-quality natural reserve of the world, located in the coasts of Chile and Argentina (Vasquez and Fonck 1993). The principal and most abundant alginate producing species in Argentina is *Macrocystis pyrifera*. Its popular name is “Cachiyuyo” in Spanish or “Kelp” in English. It forms subaquatic “forests” or

S.E. Torrusio (B)
Faculty of Natural Sciences and Museum, National University of La Plata, and National Commission of Space Activities, Argentina.
e-mail: torrusio@mail.retina.ar

X. Yang (ed.), *Remote Sensing and Geospatial Technologies for Coastal Ecosystem Assessment and Management*, Lecture Notes in Geoinformation and Cartography,
DOI 10.1007/978-3-540-88183-4 12, c Springer-Verlag Berlin Heidelberg 2009

"prairies" along the coasts in the Patagonia region, which are considered as true fauna reservoirs and can provide potential stock for deriving industrial algae products. In Argentina, the algae extraction is concentrated in Chubut and Santa Cruz, between 42°S and 52°S, at the north of Tierra del Fuego (53°S–55°S).

Several works evaluated the average biomass and density (e.g. Alveal et al. 1973, Barrales and Lobban 1975, Santelices and Lopehandía 1981, Boraso de Zaixso et al. 1983, Werlinger and Alveal 1988), but most of them did not address the spatial and temporal distribution of algae. Another problem is that as the methods they used are not compatible so that a comparison among different sites is difficult. Therefore, it is urgent to evaluate the populations of macroalgae at appropriate temporal and spatial scales with standard and systematic methods.

Many studies were conducted in different regions of the world to identify aquatic macrophytes by using remote sensing (Lambert et al. 1987, Lavoi et al. 1987, Ritter and Lanzer 1997, Steeves et al. 1991, Veisze et al. 1999, Wittlinger and Zimmerman 2001, Dierssen et al. 2003, Fyfe 2003, Vahtmäe et al. 2006, Nezlin et al. 2007, Tignyt et al. 2007). Aerospace remote sensing can provide repetitive, multispectral and synoptic data, and thus can be quite useful for coastal studies (Lamaro et al. in press).

The aims of this project were to map the spatio-temporal distribution of algae using remotely sensed data and to evaluate the usefulness of the different types of data given the frequent cloud cover in our study site. On the average, there are only 15 sunny days per year; the winter days are very short with just between six and seven sunlight hours.

Another important consideration here is that Tierra del Fuego is rich in natural resources and contains the most extensive offshore oil-producing zone in Argentina and Chile; the knowledge of macrophyte distribution is critical for offshore oil-producing activities because it can be used to monitor oil spill. For this purpose, radar images can be very useful due to high temporal coverage, weather independence, and high sensitivity to oil slick (Catoe 1973, Bentz and Pellon De Miranda 2001, Ivanov et al. 2002, Brown and Fingas 2003, Tufte et al. 2004). However, black tones in radar images could confuse us since they could be either the area with oil spill or the area with slow wind and calm waters that produce low or null backscattering signals. In addition, coastal rocky formations, because of partially submerged with tidal waters, can form a calm water area like a pool resulting in low or null backscattering and hence dark tones in radar images. Moreover, dark tones could be caused by the existence of macrophytes floating on the open sea surface or fixed on the coastal rocky formations; both cases result in low or null backscattering signals. Therefore, understanding the algae distribution can also help improve the accuracy of oil spill monitoring in our study site.

12.2 Study Area

The Argentine Province of Tierra del Fuego is a large island shared with Chile, which is located between 52° 30'S and 55°S, and 64°W and 70°W, separated from the continent by the Magallanes Strait. The algae mapping was carried out along

Fig. 12.1 Location of the study area: Magallanes Strait and the Atlantic coast of Province of Tierra del Fuego, Argentina. Note that the shoreline in the *lower right* insert extends approximately 315 km

the eastern coast extending 315 km in the island and the southeastern extreme of the Strait (Fig. 12.1). The zone has a typical glacial landscape with many channels, fiords and small islands, and its topography is irregular. Along the Atlantic coast, rocky formations are discontinuously distributed in shallow water areas. They can be submerged or not, depending on tidal dynamic.

The climate is quite cold, with strong winds during the whole year; the rainfall decreases from west with 3500 mm per year to east with 500 mm per year. The main plant community along the western and southern portions of the island is Andinean

Patagonic Forest, and different species of *nothofagus* and *peatbogs* (moss) are abundant. In the eastern and northern sectors, the steppa dominates with sparse grasses. In both the Atlantic and Pacific coasts, there are an abundance of marine mammals, such as dolphins, whales, sea lions, seals, and aquatic birds, such as fulmars, seagulls, penguins, among others.

12.3 Materials

It was necessary to combine data from several satellite sensors for mapping the algae along the eastern coast of Tierra del Fuego. The major characteristics of satellite data we used in this project are summarized in Table 12.1.

12.3.1 SAC-C

These images were acquired by the Argentinean satellite SAC-C, with the Multispectral Medium Resolution Scanner (MMRS). SAC-C was launched in November 2000, providing data with spatial resolution of 175 m, scene swath of 360 km, five spectral bands in the visible and infrared portions of the spectrum, and temporal resolution of 16 days or less according to the latitude. In the study area it was possible to obtain images every three or six days, thus increasing the chances to obtain cloud-free data.

We were able to acquire ten cloud-free images covering the period of 2002–2004. The best band combination used for macroalgae identification was near infrared-NIR (4), shortwave infrared-SWIR (5), and red (3). The kelp forests are spectrally similar to land vegetation but with higher reflectance in the near infrared portion of the spectrum. The best band combination allows to identify and separate the kelp beds and other macrophytes from bare rocks, suspended sediments or phytoplankton components in the sea.

12.3.2 Landsat

We used data from three Landsat sennors: Multispectral Scanner (MSS), Thematic Mapper (TM), and Enhanced Thematic Mapper Plus (ETM+). We acquired one 1981 MSS scene that was originally in film with the blue (4), green (5) and near infrared (7) band combination and at the scale of 1:1000000, and later digitized using a digital camera. We obtained nine cloud-free TM images from 1999 to 2004 covering Spring, Summer and Fall months. The band combination was NIR (4), SWIR (5), and red (3), identical to the one we used for the SAC-C images: We also composed a true color image using bands red (3), green (2), and blue (1), which allowed to distinguish suspended sediments from a coastal river. We also acquired 15

Table 12.1 List of satellite images used in the study

Satellite/sensor	Path/row	Date	Spatial resolution (m)
SAC-C/(MMRS)	224	Jul. 28 2002	175
SAC-C/(MMRS)	225	Aug. 04 2002	175
SAC-C/(MMRS)	225	Sep. 05 2002	175
SAC-C/(MMRS)	225	Apr. 01 2003	175
SAC-C/(MMRS)	225	May 19 2003	175
SAC-C/(MMRS)	224	Nov. 04 2003	175
SAC-C/(MMRS)	224	Jan 23 2004	175
SAC-C/(MMRS)	224	Feb. 08 2004	175
SAC-C/(MMRS)	225	Feb 15 2004	175
SAC-C/(MMRS)	225	Mar. 18 2004	175
Landsat 5 TM	225/98	Mar. 13 1999	30
Landsat 5 TM	224/98	Oct. 27 2003	30
Landsat 5 TM	225/98	Nov. 03 2003	30
Landsat 5 TM	225/98	Dec. 05 2003	30
Landsat 5 TM	223/98	Jan. 24 2004	30
Landsat 5 TM	225/98	Feb 07 2004	30
Landsat 5 TM	223/98	Mar. 12 2004	30
Landsat 5 TM	224/98	Mar. 19 2004	30
Landsat 5 TM	224/98	Apr. 04 2004	30
Landsat 7 ETM+	226/97	Aug. 24 2001	30
Landsat 7 ETM+	226/97/98	Oct. 17 2003	30
Landsat 7 ETM+	224/98	Oct. 19 2003	30
Landsat 7 ETM+	224/97	Nov. 04 2003	30
Landsat 7 ETM+	224/97/98	Jan. 07 2004	30
Landsat 7 ETM+	224/97	Jan. 23 2004	30
Landsat 7 ETM+	225/97/98	Feb.15 2004	30
Landsat 7 ETM+	225/98	Mar. 02 2004	30
Landsat 7 ETM+	226/97	Mar. 09 2004	30
Landsat 7 ETM+	226/98	Mar. 25 2004	30
Landsat 7 ETM+	225/97	May. 05 2004	30
Landsat 7 ETM+	225/98	May. 05 2004	30
Terra/Aster-VNIR	226/98	Oct. 18 2006	15
Quick Bird	–	Feb. 06 2005	2.5
Quick Bird	–	Feb. 27 2004	2.5
Quick Bird	–	Dec. 25 2002	2.5
Radarsat/Beam Mode W1	Ascend. orbit	Apr. 06 2007	30
Radarsat/Beam Mode SNA	Descend. orbit	May. 23 2006	50

cloud-free ETM+ images from 2001 to 2004. The band combination more adequate to identify the algae was NIR (4), SWIR (5), and red (3).

12.3.3 ASTER

We acquired one image in Spring 2006 from the Advanced Spaceborne Thermal Emission and Reflection Radiometer (ASTER) on the Terra satellite, which covers a small portion of the coast. With a swath of 60 km, ASTER has 15 bands, including three visible and near infrared bands with 15 m spatial resolution and 8-bit radiometric resolution, a second near infrared backward-scanning band used to create a stereo view, six SWIR bands with 30 m spatial resolution and 8-bit radiometric resolution, and five thermal bands (TIR) with 90 m spatial resolution and 16-bit radiometric resolution. The band combination we used was NIR (3), red (2), and green (1); these bands have 15 m spatial resolution, allowing to identify different macrophytes communities and determine the phenological state with textures and tones.

12.3.4 QuickBird

We used three QuickBird multispectral images with very high spatial resolution, which cover part of the eastern coast of Tierra del Fuego and the Magallanes Strait for Spring 2002, Summer 2004 and Summer 2005. They allowed us to compare the current algae distribution with historical data.

12.3.5 Radarsat

Radarsat's SAR (synthetic aperture radar) is an active sensor. It transmits a microwave energy pulse directly towards the Earth's surface. The SAR sensor measures the amount of energy which returns to the satellite after it interacts with the Earth's surface. Unlike optical sensors, the microwave energy penetrates clouds, rain, dust, or haze, and acquires images independent of the Sun and the weather conditions. Variations in the returned signal are the result of changes in the surface roughness and topography as well as physical properties such a moisture content and electrical properties (Radarsat User Guide 1995). There are several products with different spatial resolution according to the beam modes.

We acquired two Radarsat images: Scan Narrow A with 29° incidence angle, spatial resolution of 50 m, and 200 km swath for 23 May 2006; Wide 1 with 24° incidence angle, spatial resolution of 30 m, and 150 km swath for 6 April 2007. For oil spill detection, steep incidence angles are preferred. The SAR data were processed with the adaptative filters of Lee for the Scan Narrow A mode and Frost for the Wide 1 mode to suppress the image speckles for improving the visual interpretability.

The Radarsat images were used to analyze "black areas" and to separate the different features on or near the sea surface: area with low/null wind speed, inland waters, and emergent or floating kelps from real or potential oil spill. They also allow to view some offshore oil platforms that are hardly seen with medium-resolution optical data.

12.3.6 Other Data

We also analyzed historical aerial photographs and bathymetric maps covering part of Tierra del Fuego. These materials were produced by the Naval Hydrographical

Survey. We considered four aerial photos from 1970 at the scale of 1:20000. The bathymetric map was from 1939 at the scale of 1:400000.

12.4 Methods

Mapping of the marine macrophyte communities in the entire study area was carried out by using the optical data from SAC-C and Landsat TM/ETM+. We clipped most of the images to focus on the coastal area of interest only; this could also help offset data processing burden. We georeferenced all the image subsets into geographic coordinates, WGS84 datum and ellipsoid. The resampling method used was cubic convolution and the average RMS was about one pixel for every image. For the SAC-C images the mean RMS was 98.4 m, and 35 ground control points (GCP) were used; for the Landsat images, the mean RMS was 17.8 m, and 23 GCPs were used; and for the ASTER images, the mean RMS was 10.4 m, and 18 GCPs were used.

Both digital and visual analysis methods were combined to mutually maximize their capability for algae community identification. Because the weather and tidal conditions were various for each optical image, we tried different methods to distinguish the macrophytes. Firstly, we tested supervised and unsupervised classifiers, but the spectral confusion among some classes made difficult to obtain accurate results. Then, we conducted spectral enhancement to maximize the visual separability considering colors, tones, textures and shapes of the submerged vegetation along the coast. Specifically, we applied linear stretching, Gaussian, histogram equalization, standard deviations, interactive stretching, and band ratio to different images in order to improve the algae recognition. With the enhanced images, we further mapped the algae communities by using on-screen digitizing, and the derived maps were managed with a geographic information system.

The aerial photos were co-registered and mosaicked. The bathymetric map was co-registered too. A detailed visual analysis was done using the photos and the satellite images discussed in Sect. 12.3. This visual interpretation allowed us to analyze the temporal and spatial changes and to compare the contributions and/or disadvantages of each sensor.

All the above data processing tasks were conducted by using ERDAR Imagine 8.4, ENVI 3.5 and Arcview 3.1.

12.5 Results

The final maps show that the marine macrophytes were discontinuously distributed along the eastern coast of Tierra del Fuego (Fig. 12.2a,b). This distribution pattern may be related to the tidal influence and the type of rocks where the plants can fix. As for the seasonal variation, we did not find any significant difference between

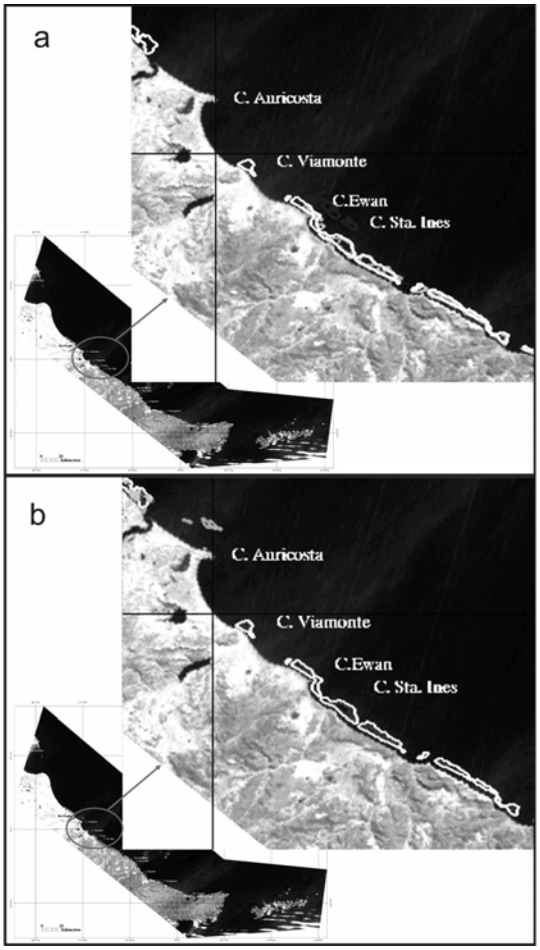

Fig. 12.2 Seasonal algae distribution: (**a**) Interpretation from the Spring-Summer Landsat and SAC-C images overlaid on a SAC-C image. Note that the white polygons are the distribution of algae; (**b**) Interpretation from the Fall-Winter Landsat and SAC-C images overlaid on a SAC-C image. Note that the white polygons are the distribution of algae

Fall-Winter and Spring-Summer covers for the period of 1999–2004 (Fig. 12.2a,b). We believe that some field verifications by experts in algae and remote sensing around the year should help improve the mapping accuracy.

From Fig. 12.3, we can see three portions of the 1939 bathymetric map with the presence of algae in the same location where we can find them in recent satellite images, e.g. the Landsat 5 TM scene acquired on November 2003. In the same way we also compare the aerial photos mosaic (1970) versus Quick Bird (2002) (Fig. 12.4), and Landsat 2 MSS (1981) versus SAC-C (Fig. 12.5).

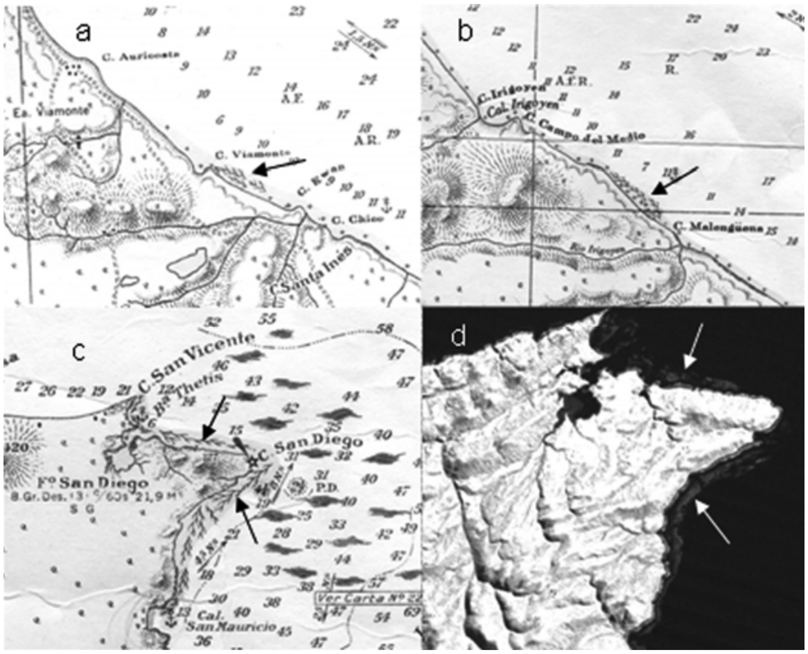

Fig. 12.3 Bathymetric maps for the three sites (**a, b, and c**) along the eastern coast of Tierra del Fuego and the south extreme of the island. Note that (**d**) is part of the near infrared band of a Landsat 5 TM image acquired on November 2003, covering the same area as (**c**) does. The algae locations are indicated with *arrows*

Note that from the ASTER image (Fig. 12.6a) different marine macrophyte communities, such as *Macrocystis pyrifera* (Fig. 12.6b,c), can be observed with various reddish colors. Figure 12.6c,d are the outputs of different enhancements on a Landsat 5 TM image acquired on November 2003 with two different band combinations: (a) 3,2,1 (Fig. 12.6d) allowing to identify a sediments plume (in beige-yellowish color); and (b) 4,5,3 (Fig. 12.6e) permitting to identify macroalgae (in purplish color).

Several additional figures helped us to assess the contribution of radar images for algae identification and to explain how we separated and analyzed dark zones. Figure 12.7 is a 2004 Radarsat Scan Narrow A image on which we see some bright spots indicating offshore oil platforms in the Magallanes Strait and Northeast of Tierra del Fuego. In Fig. 12.8, we can see some black areas in the 2007 Radarsat image, which were with slow wind and calm water; we see some floating kelps (indicated with the white arrows) from the 2004 QuickBird image, which were over the same areas showing in black from the 2007 Radarsat image. In Fig. 12.9 we can see some partially submerged rocks in the 2004 Scan Narrow A Radarsat image (in dark tones) (Fig. 12.9a) and some offshore oil-platforms (Fig. 12.9b). Note from the

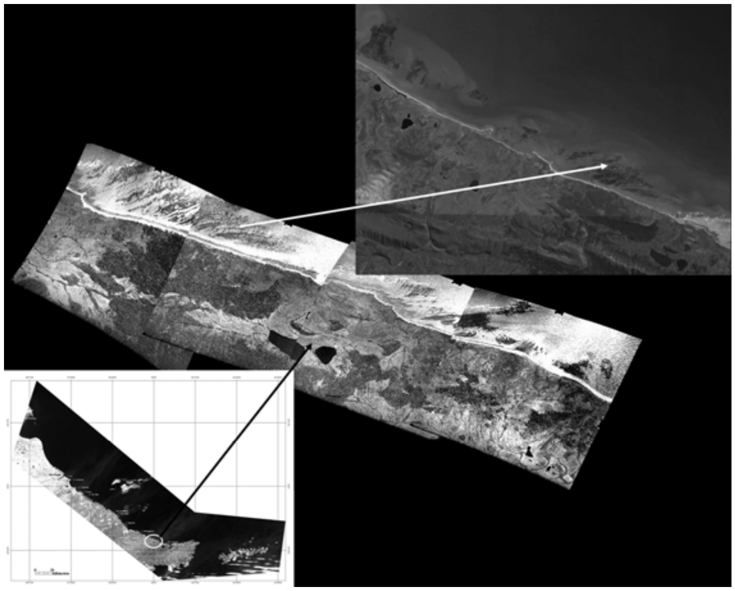

Fig. 12.4 Comparison between a 1970 aerial photos mosaic (*centre*) and a 2002 QuickBird image (the *upper right* insert). The algae locations are indicated with the white *arrow*

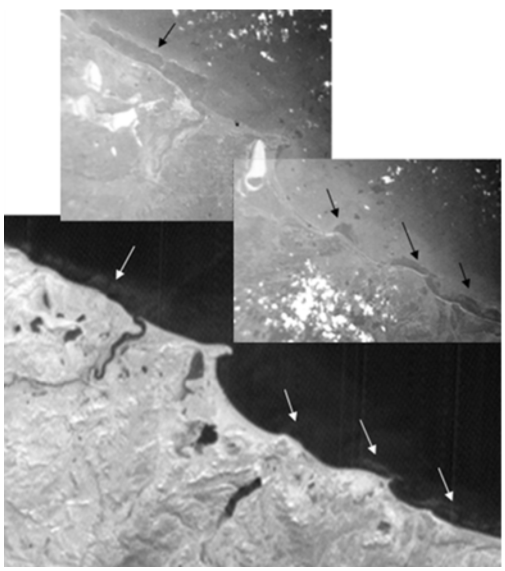

Fig. 12.5 Comparison between the images from Landsat 2 MSS (1981) (the *two upper* figures) and from SAC-C (September 2002)

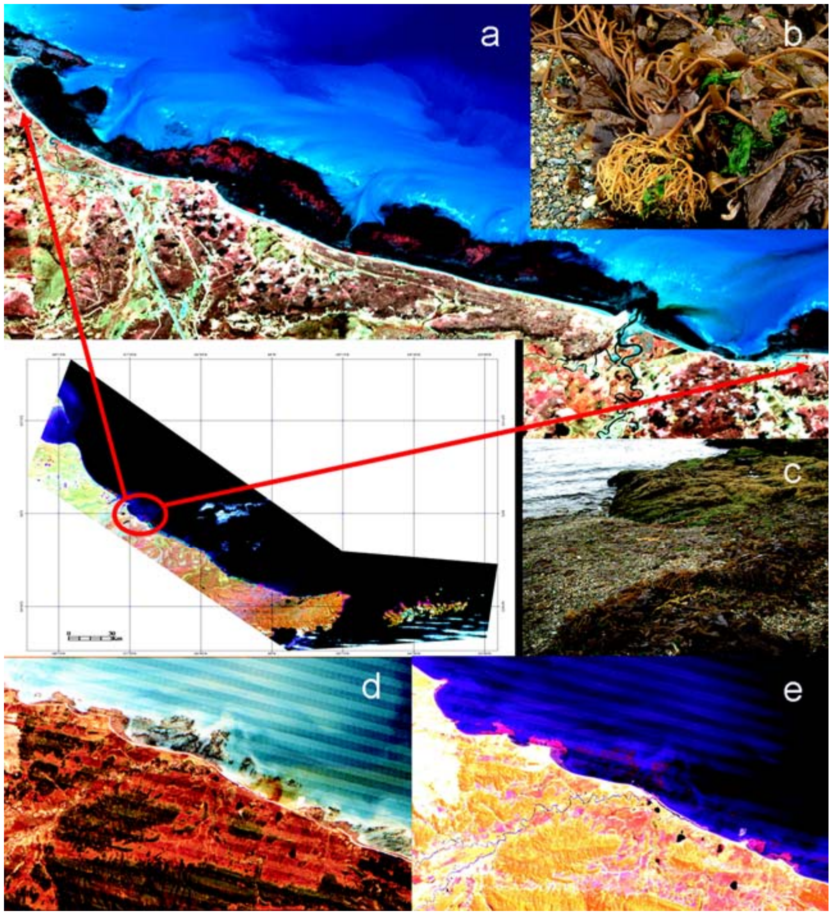

Fig. 12.6 (**a**) An ASTER image acquired on October 2006 showing algae in reddish tones on rocks. *Macrocystis pyrifera* on the rocks (**b**) and on the fixer disc (**c**). Color composites of the 2003 Landsat 5 TM image: (**d**) with bands 321; a sediments plume develops in the lower right portion; and (**e**) with bands 453; this sediment plume is not visible and algae are in purplish

April 2006 Landsat 5 TM image, these areas emerged without plants (Fig. 12.9e). Similar comparison is shown in Fig. 12.9d between the 2007 radar and the 2004 QuickBird images (Fig. 12.9c) in the northern island; coastal areas with dark tones are calm water without fixed algae but with floating kelps near the shoreline.

In general we found that the macroalgal distribution did not change much over time considering the materials we used covered the period of 1939–2007. Moreover, the use of different sensors, both optical and active, helped improve the possibilities of obtaining cloud-free images, and thus promoting our inventory effort in this area where this type of information was sketchy and sometimes absent.

Fig. 12.7 Part of the Radarsat image (Scan Narrow A, May 2004) covering the Magallanes Strait. Note that the bright spots indicate off-shore oil platforms

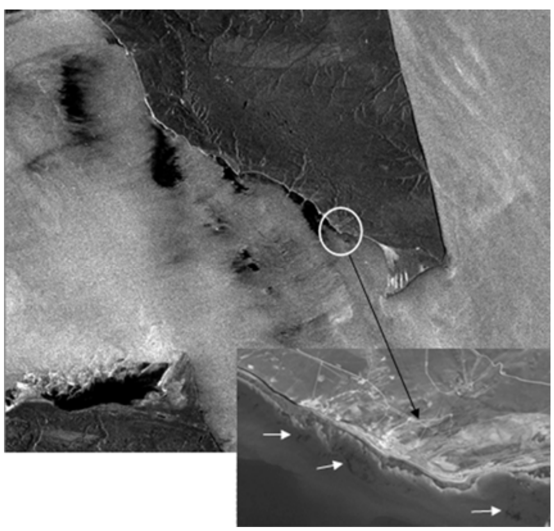

Fig. 12.8 Part of the Radarsat image (Wide 1, Apr. 2007) covering the Magallanes Strait; dark areas are with slow wind and calm water. Part of the QuickBird image (the *lower right* insert) shows some floating seagrasses, which are indicated with three white *arrows*

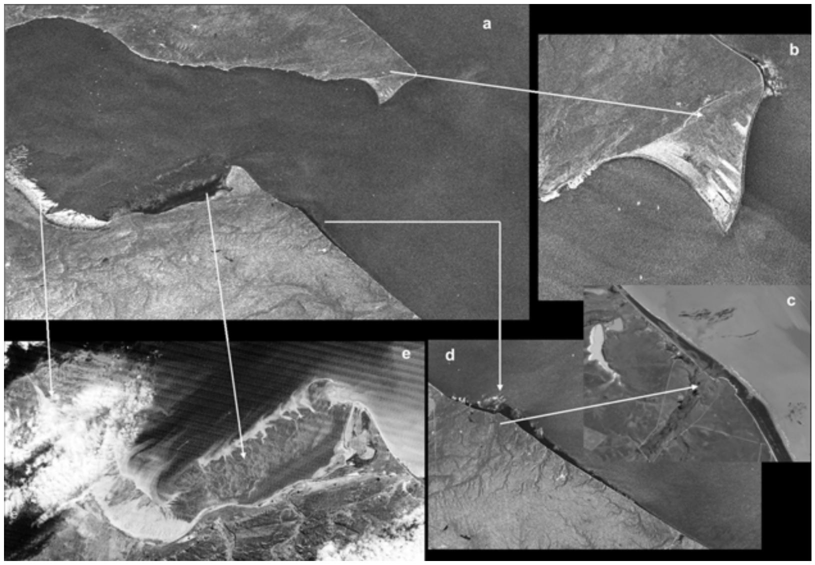

Fig. 12.9 Partially submerged rocks (in dark tones) on the radar image (Scan Narrow A 2004): (**a**) in the bay and (**b**) an enlargement to show some oil-platforms. (**e**) Part of the 2006 Landsat 5 TM image (original in color, displayed with bands 321) shows the same area that emerged without plants. Comparison between the 2007 radar (**d**) and the 2004 QuickBird (**c**) images shows that some floating algae rather than fixed ones are in the coastal areas with dark tones

12.6 Conclusions

Probably, the comparison among different satellite sensors and other sources of data was the most interesting aspect in this project. This study offers an insight concerning the advantages and combinations of several products for mapping natural resources, algae in this case. The use of these tools allows to obtain an integral perspective. We considered the advantages of using optical data with different spatial resolution to identify the current macroalgae distribution and to detect potential seasonal changes. On the other hand, the use of other data sources, such as historic bathymetric maps and aerial photographs, allowed us to map the spatial distribution of algae in the past. These have been very helpful to examine the temporal changes through several decades.

Considering the application of active remote sensor data in this study we should emphasize their advantage when there is frequent cloud cover during the year in our study area. Because of the existence of intensive offshore oil-producing activities, however, the radar images play a critical role in every segment of the environmental monitoring. Our results showed that it is not easy to separate among calm water areas, macroalgae communities, and oil spills by using active remote sensing alone. Thus, it would be very useful to construct a complete kelp bed data base for

Argentina's southern coast by combining both optical and radar data; we believe such database will help us to produce better results, and thus improving our oil spill monitoring plan.

Given the above considerations, we believe that the construction of the algae distribution base maps covering the 315 km coast is economically and environmentally important. We should incorporate this mapping effort into our coastal monitoring and management plans.

Acknowledgements I would like to thank National Commission of Space Activities (CONAE) for providing the valuable images used in this project. A very special acknowledgment to M.A. Geology Mr. J. Ulibarrena, to my advanced student Ms. J. Otero and to Mr. G. Weber, the computer operator, for their collaboration in the mapping of these algae. Besides, I thank Dr. C. Moyano, Dr. E. Baran, and several colleagues for the critical reading of the manuscript.

References

Alveal K, Romo H, Valenzuela J (1973) Consideraciones ecológicas de las regiones de Valparaíso y de Magallanes. Rev Biol Mar 15:1–29

Barrales H, Lobban CS (1975) The comparative ecology of Macrocystis pyrifera, wit emphasis in the forest of Chubut, Argentina. J Ecol 63:657–677

Bentz CM, Pellon De Miranda F (2001) Application of remote sensing data for oil spill. Monitoring in the Guanabara Bay, Rio de Janeiro, Brazil. Anais X SBSR, Foz do Iguaçu, April 21–26, INPE, pp 747–752

Boraso de Zaixso AL, Piriz ML, Romanello EE (1983) Posibilidades de desarrollo de la industria alguera en la Prov. de Santa Cruz (República Argentina). Informe Proyecto "Cinco Provincias Argentinas", OEA

Brown CE, Fingas MF (2003) Synthetic Aperture Radar Sensors: Viable for Marine Oil Spill Response? Emergencies Science and Technology Division Environment Canada. http://www.ecy.wa.gov/programs/spills/response/taskforce/AMOP%202003%20SAR%20Oil%20Spills.pdf (Last access on 16 June 2006)

Catoe C (1973) Remote Sensing Techniques for Detecting Oil Slicks. J Petrol Technol 25:267–278

Dayton PK (1985) The structure and regulation of some South American kelps communities. Ecol Monogr 55:447–468

Dierssen HM, Zimmennan RC, Leathers RA, Downes TV, Davis CO (2003) Ocean color remote sensing of seagrass and bathymetry in the Bahamas Banks by high resolution airborne imagery. Limnol Oceanogr 48:444–455

Fyfe SK (2003) Spatial and temporal variation in spectral reflectance: Are seagrass species spectrally distinct? Limnol Oceanogr 48:464–479

Ivanov A, He M, Fang M (2002) Oil spill detection with the RADARSAT SAR in the waters of the Yellow and East China Sea: A case study. http://www.gisdevelopment.net/aars/acrs/2002/sar/011.pdf (Last access on 16 June 2006)

Lamaro A, Torrusio S, Ulibarrena J, Mugni H, Bonetto C. Mapping of Coastal Changes Applying Maps, Satellite Images and GIS in Samborombón Bay, Argentina. Int J Ecol Dev (in press)

Lambert E, Dubois JM, Lavoi A, Grenier M (1987) Remote sensing of marine macrophytes. Photo Interprétation 1:1–8

Lavoi A, Lambert E, Dubois JM, Gendron L (1987) Sensing and mapping of Laminaria of the Coast of Quebec and biomass evaluation. Photo Interprétation 1:9–16

MacDonald, Dettwiler and Associates Ltd (1995) Radarsat user guide p 113

Nezlin NP, Kamer K, Stein ED (2007) Application of Color Infrared Aerial Photography to Assess Macroalgal Distribution in an Eutrophic Estuary, Upper Newport Bay, California. Estuaries and Coasts 30:855–868

Rees WM (1986) Alginate marketing in the 1980's. Monografías Biológicas (Chile) 4:13–28

Ritter R, Lanzer EL (1997) Remote Sensing of Nearshore Vegetation in Washington State's Puget Sound. Proceedings of 1997 Geospatial Conference, vol 3. Seattle, WA, pp 527–536

Santelices B, Lopehandía J (1981) Chilean seaweeds resources: A quantitative review of potential and present utilization. Int Seaweed Symp 10:725–730

Steeves P, Waldron MC, Finn JT (1991) Aquatic Macrophyte Mapping Using Thematic Mapper Imagery and a Geographic Information System. ESRI Users Conference in San Diego, California. http://ma.water.usgs.gov/publications/ja/lakes_ponds_journal.htm (Last access on 20 November 2007)

Tignyt V, Ozer A, De Falcot G, Baroli M, Djenidi S (2007) Relationship between the Evolution of the Shoreline and the Posidonia oceanica Meadow Limit in a Sardinian Coastal Zone. J Coastal Res 23:787–793

Tufte L, Trieschmann O, Hunsänger T, Kranz S, Barjenbruch U (2004) Using air- and spaceborne remote sensing data for the operational oil spill monitoring of the german north sea and Baltic sea. http://www.isprs.org/istanbul2004/comm7/papers/193.pdf (last access on 16 June 2006)

Vahtmäe E, Kutser T, Martin G, Kotta J (2006) Feasibility of hyperspectral remote sensing for mapping benthic macroalgal cover in turbid coastal waters: a Baltic Sea case study. Remote Sens Environ 101:342–351

Vasquez JA, Fonck EA (1993) Estado actual y perspectivas de la explotación de algas alginofitas en Sudamerica. In: Zertuche Gonzalez JA (ed) Situacion actual de la industria de macroalgas productoras de ficocoloides en América latina y el Caribe, Project reports No.13, FAO Italy, p 66

Veisze P, Kilgore A, Mark Lampinen M (1999) Building a California Kelp Database Using GIS. http://www.imaging.geocomm.com/features/californiakelp (Last access on 20 November 2007) Werlinger C, Alveal K (1988) Evaluación de algas en ambientes restringidos del Golfo de Arauco(Chile): Punta Fuerte Viejo a Río Tubul. Guayana Bot 45:461–474

Wittlinger SK, Zimmerman RC (2001) Hyperspectral remote sensing of subtidal macrophytes in optically shallow water. Aquatic Sciences Meeting, Albuquerque. http://www.aslo.org/albuquerque2001/507.html (Last access on 25 March 2008)